Electronic Supplementary Material (ESI) for New Journal of Chemistry.

Support information

Efficient Photocatalytic Performance and Mechanism of Copper(I) Metal–Organic Framework Nanosheets

Shaolong Yang[1,2], Yuhuan Chen[1], Shixiong Li[1,2*], Huijun Chen[3*]

[1]School of Mechanical and Resource Engineering, Wuzhou University, Wuzhou 543002, P. R. China

[2]School of Chemistry and Chemical Engineering, Guangxi University, Nanning, 530004, P. R. China

[3]School of Food and Pharmaceutical Engineering, Wuzhou University, Wuzhou 543002, P. R. China

*E-mail:lsx1324@163.com; chj_chem@163.com

Contents

Instrument and characterization analysis conditions

The IR spectra of **1** was measured on a Nicolet 5DX FT-IR spectrometer withKBr pellets . The Elemental analysis (carbon, hydrogen, and nitrogen) of **1** was performed with a Perkin-Elmer 240 elemental analyzer. The X-ray powder diffraction of **1** was carried out using Rigaku's D/max 2500 X-ray diffractometer with Cu Kα radiation (λ = 0.15604 nm); the tube voltage was 40 kV, the tube current was 150 mA, a graphite monochromator was used, and 2θ was 5° to 50º. The X-ray crystallography of **1** was collected on a Bruker Apex CCD area-detector diffractometer. The X-ray photoelectron spectroscopy (XPS) of **1** was performed on a Kratos Axis Ultra DLD system with a base pressure of 10^{-9} Torr. The scanning electron microscopy (SEM) of **1** was performed by using the Hitachi S-4800 under the following conditions: Mag.: 1 KX, Signal A: VPSE, and EHT: 20 kV. The surface area of **1** was determined using BET technique; the apparatus (AutoChem II 2920) was employed to determine the surface area of the **1** using N_2 as the probe gas. The UV-Vis diffuse reflectance spectra of P_{25} and **1** were measured by a UV-2700 instrument from Shimadzu of Japan with $BaSO_4$ as a reference. The electrochemical cyclic voltammetry of **1** was conducted on a CHI 410B Electrochemical Workstation with Pt disk coated with the polymer film, Pt plate, and Ag/Ag^+ electrode as working electrode, counter electrode, and reference electrode respectively in a 0.1 mol/L tetrabutylammonium hexafluorophosphate (Bu_4NPF_6) acetonitrile solution. The electrochemical potential was calibrated against Fc/Fc^+. Measure the pH value in the solution by using the Mettler FE28 Standard pH meter. The concentration of MB and MO in solution were measured with UV-Vis 2550 in 664 nm and 466 nm wavelength, respectively.

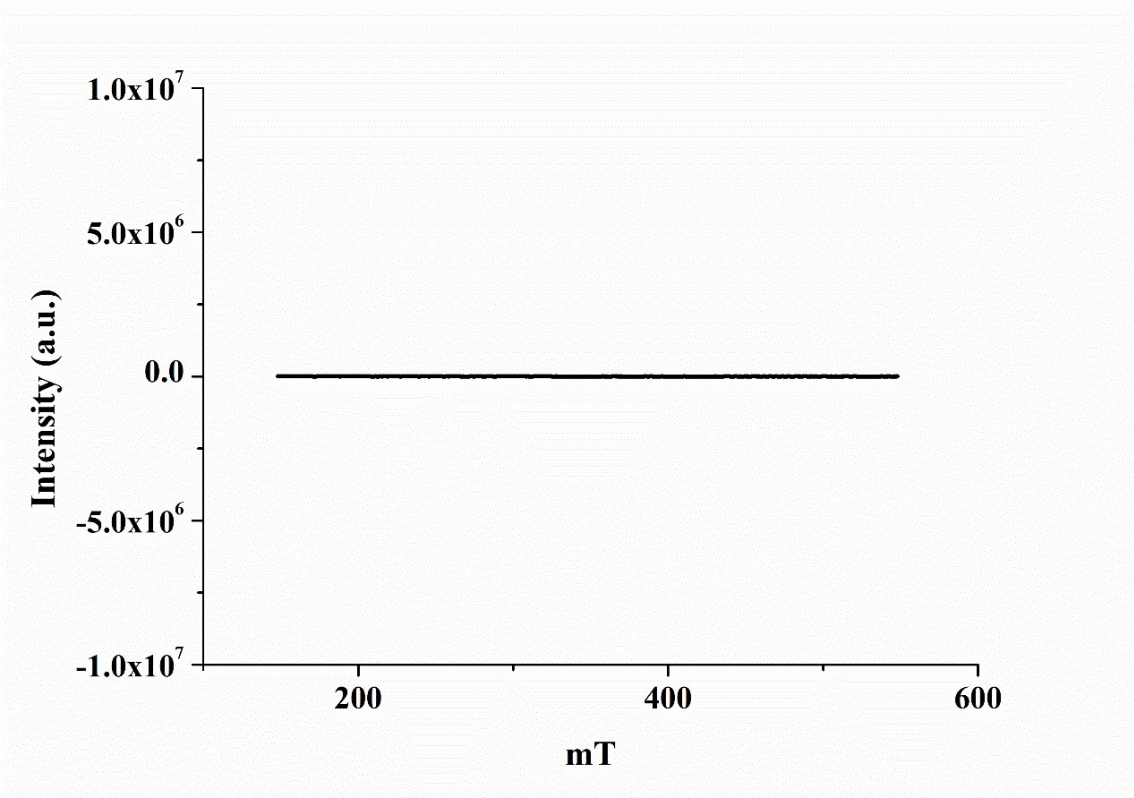

Figure S1. The EPR of **1**.

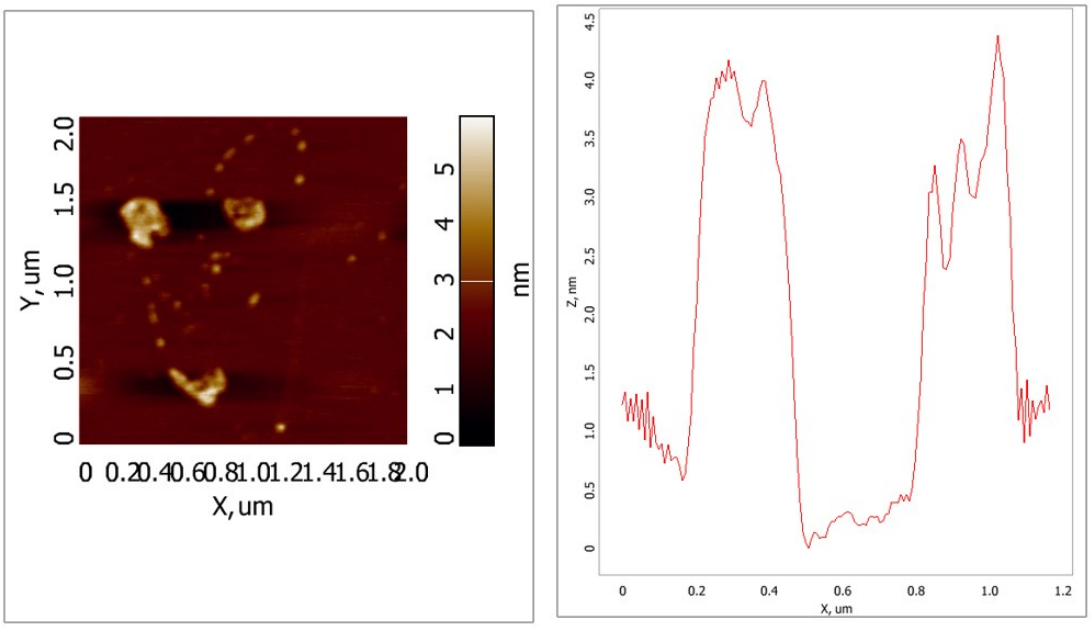

(a) **(b)**

Figure S2. (a) and (b) AFM of nanosheets.

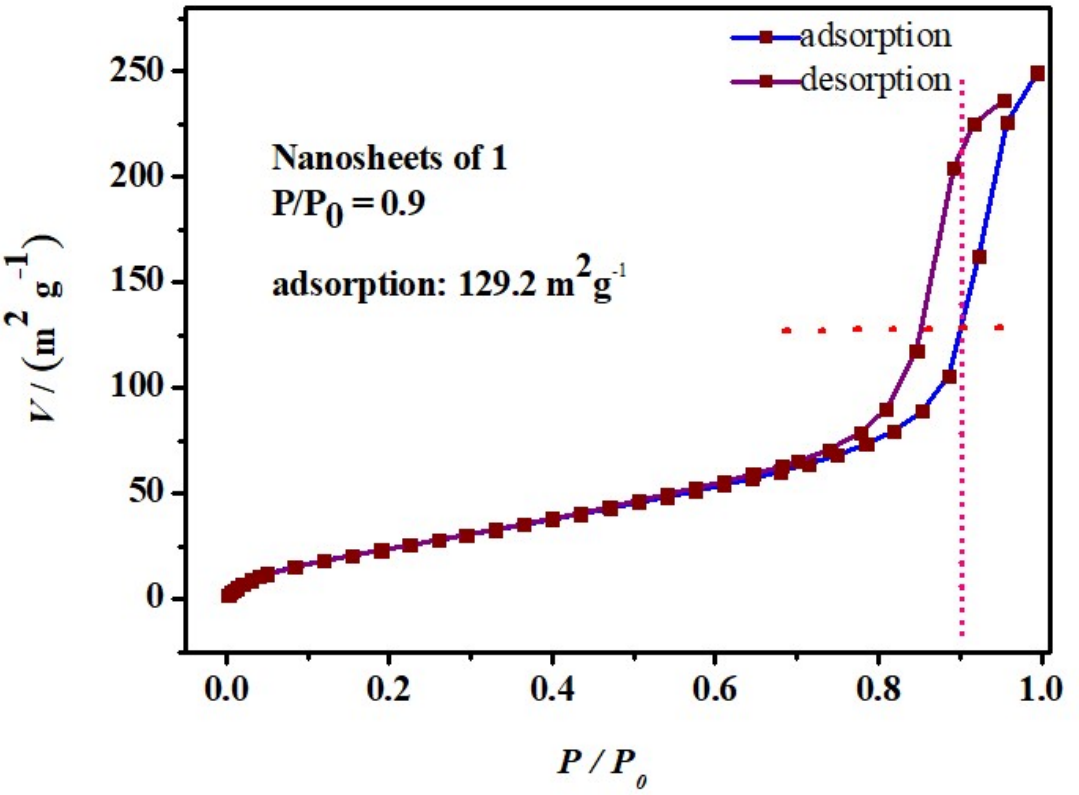

Figure S3. N_2 adsorption/desorption isotherm of nanosheets.

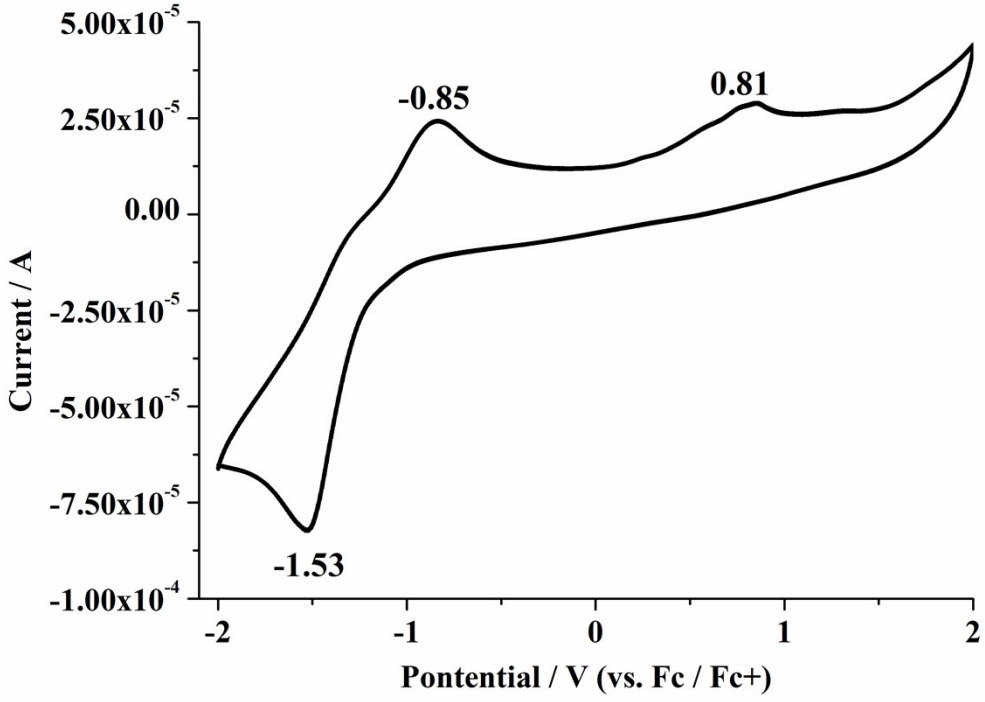

Fihure S4. Cyclic voltammetry curve of nanosheets.

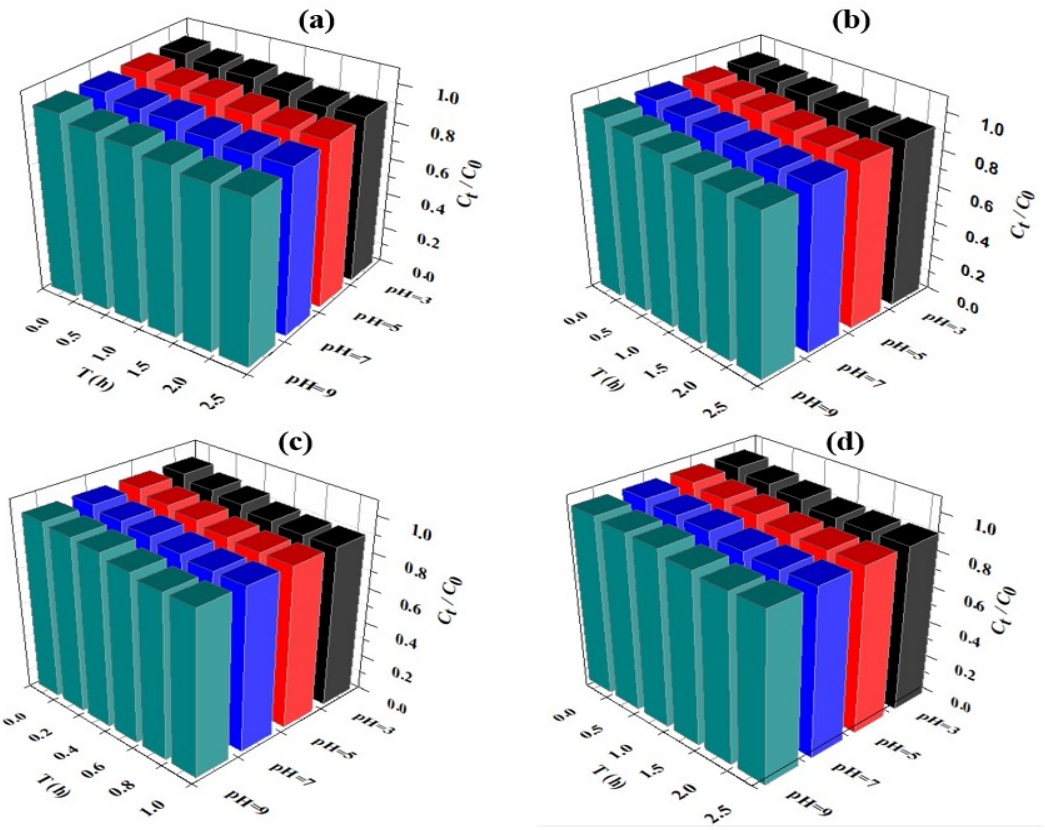

Figure S5. Adsorption performance: (a) and (b) adsorption properties of MB by nanosheets, and P_{25}, respectively; (c) and (d) adsorption properties of MO by nanosheets, and P_{25}, respectively.

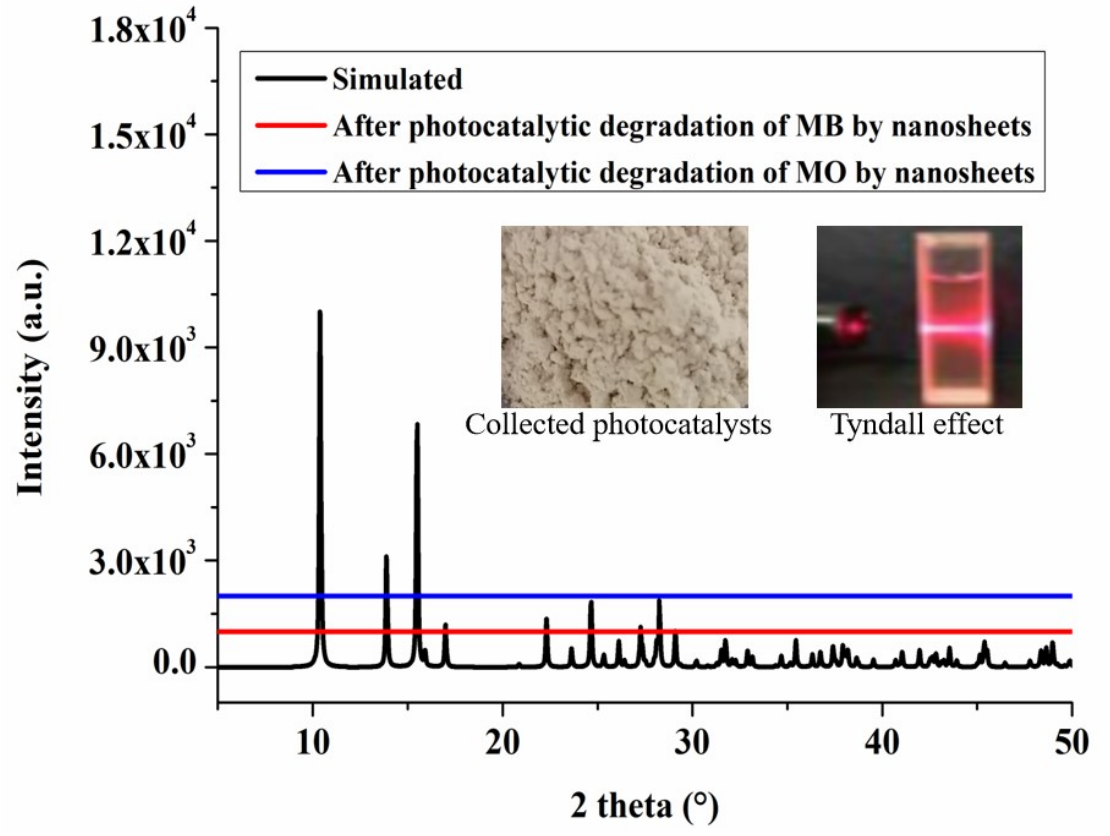

Figure S6. XRD of nanosheets after photocatalytic degradation of MB and MO.

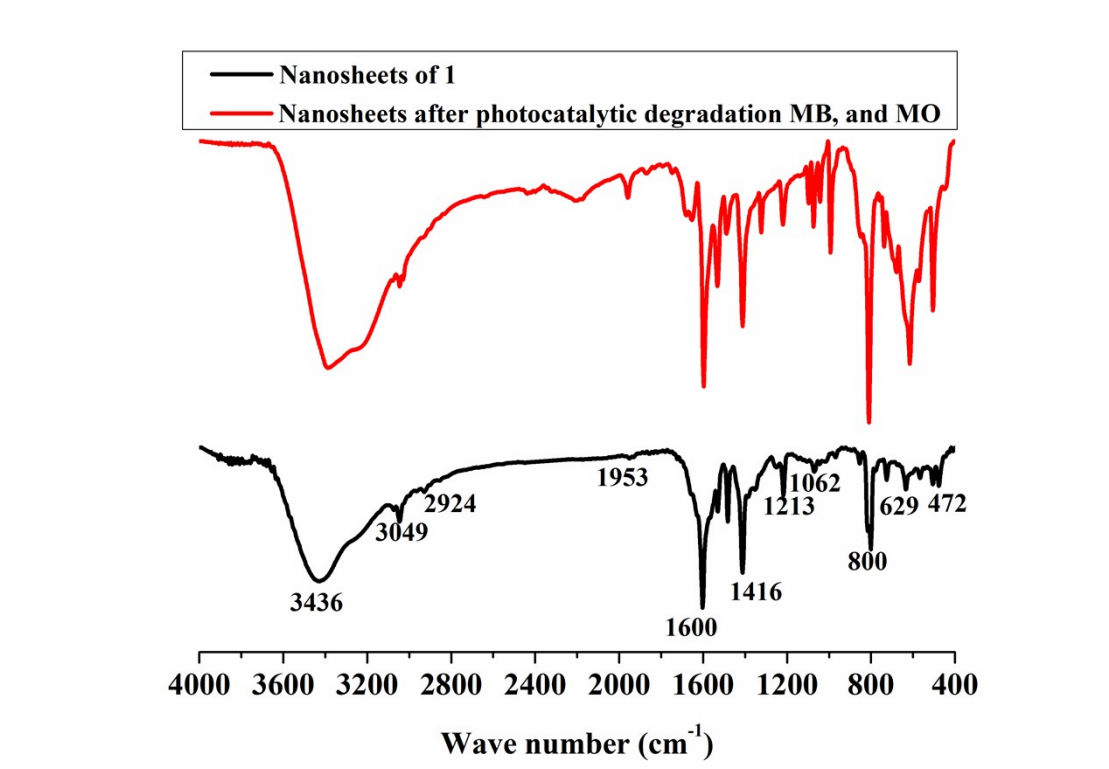

Figure S7. IR of nanosheets after photocatalytic degradation of MB, and MO.

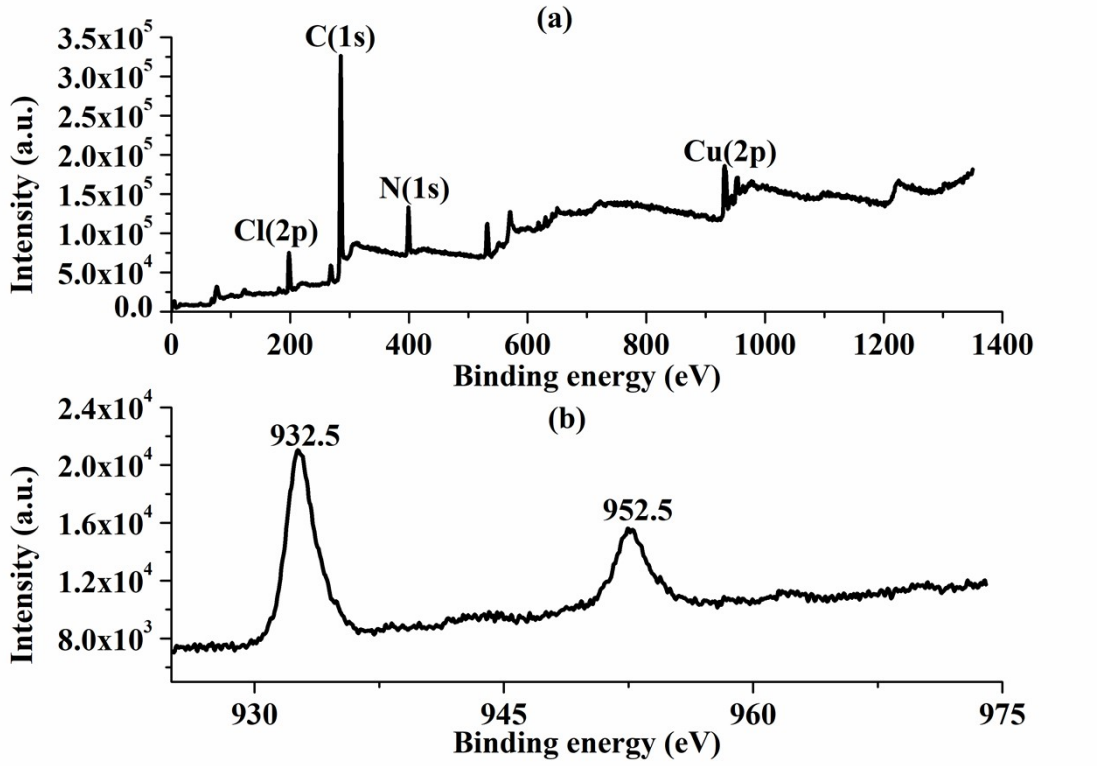

Figure S8. XPS of nanosheets after photocatalytic degradation of MB, and MO.

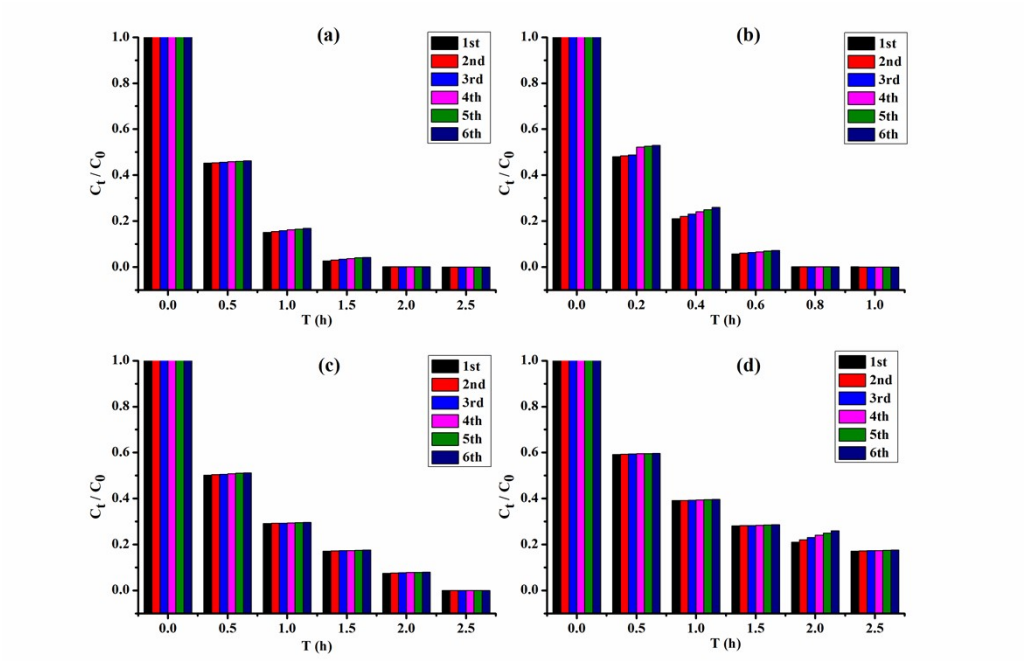

Figure S9. (a) And (b) are the cyclic experiments of nanosheets photocatalytic MB and MO, respectively; (c) and (d) are the cyclic experiments of P_{25} photocatalytic MB and MO, respectively.

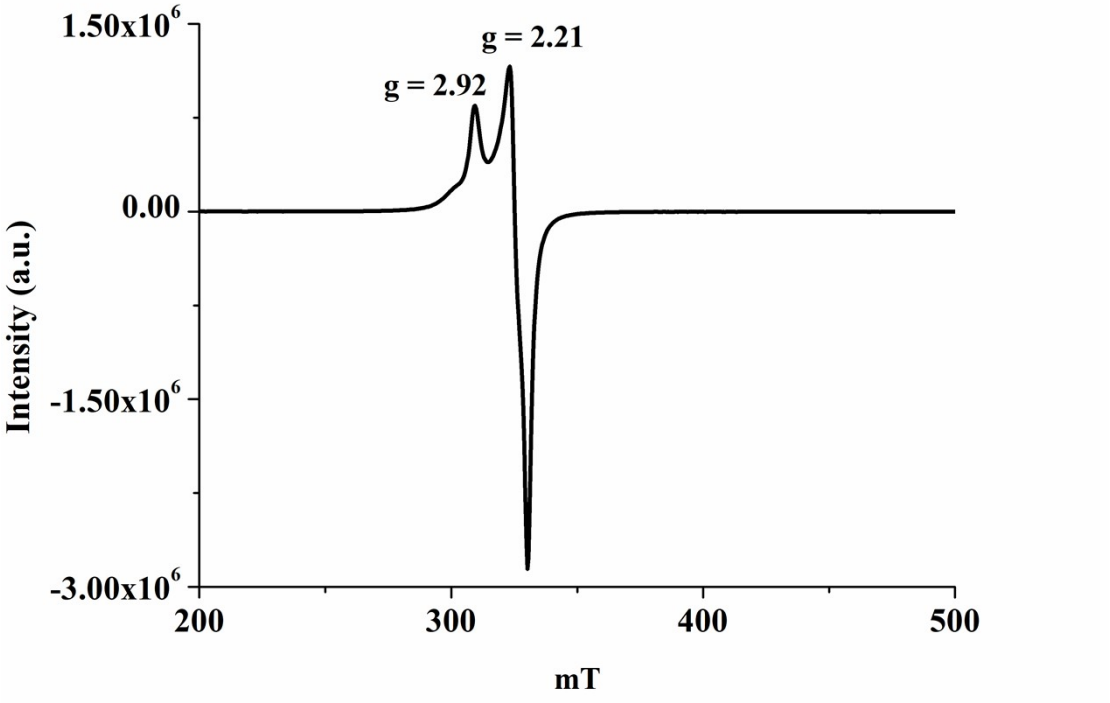

Figure S10. *In-situ* EPR spectrum of nanosheets sample under 175 W high-pressure mercury lamp radiation catalyzed the MB at 173 K.

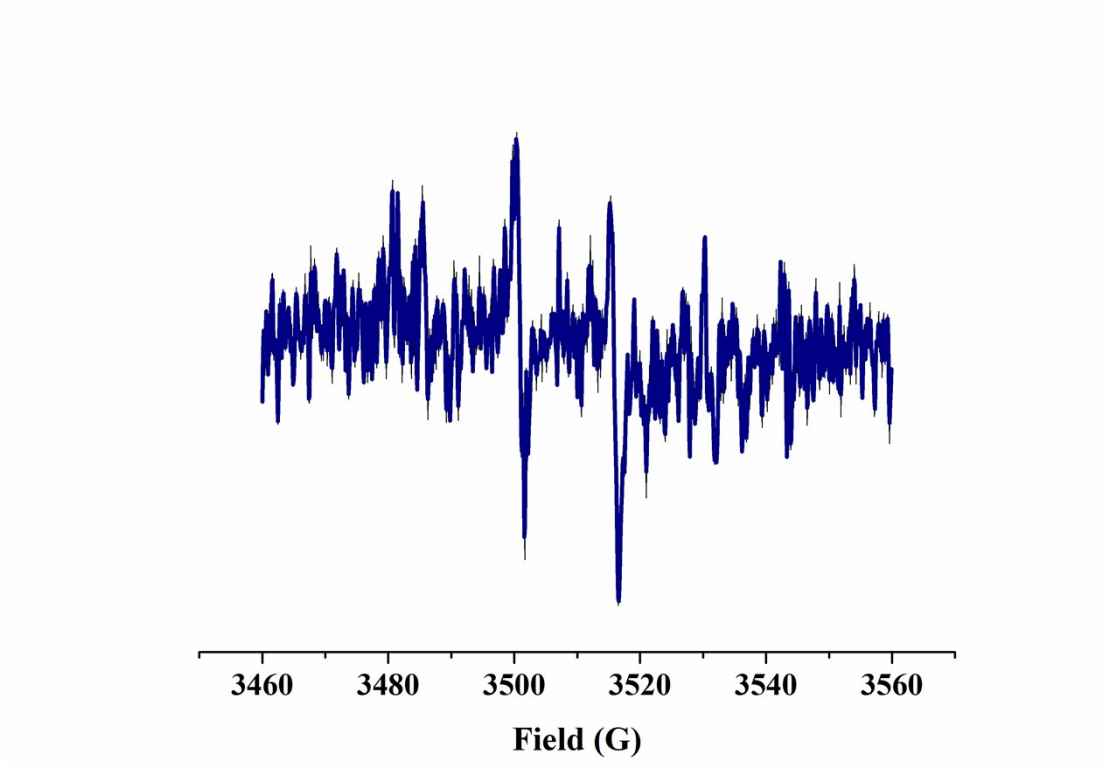

Figure S11. The ·OH active species captured by EPR.

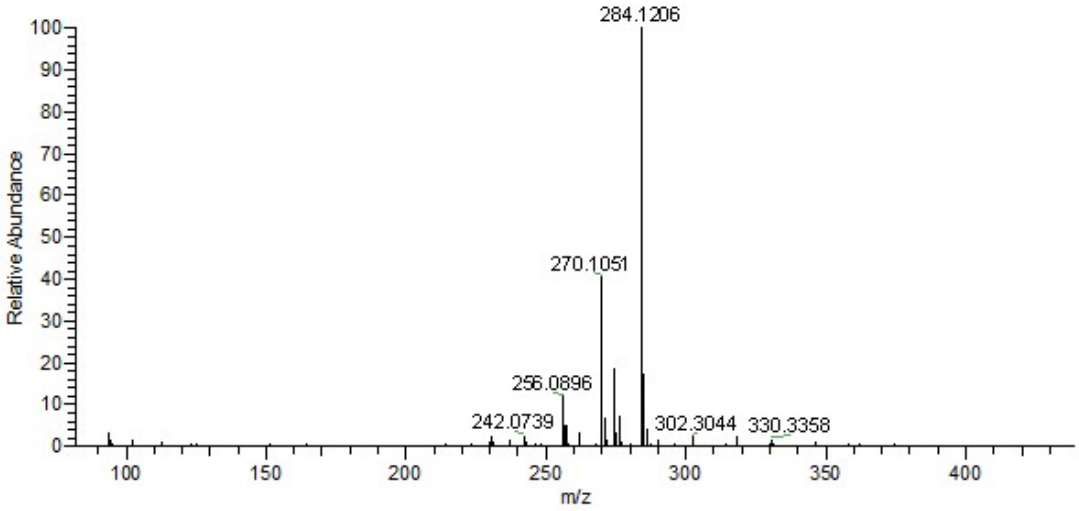

Figure S12. ESI-MS test and analysis of MB solution during photocatalytic process.

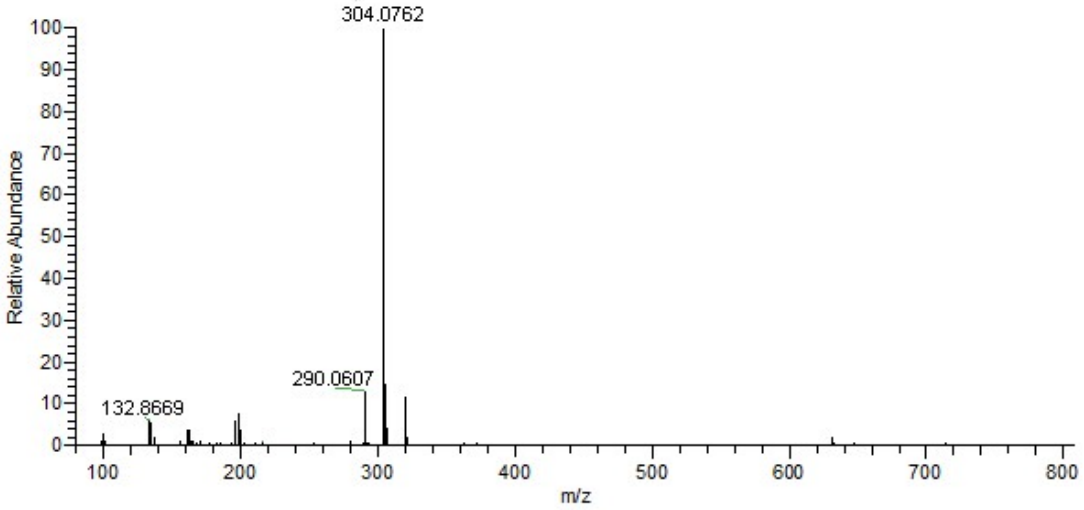

Figure S13. ESI-MS test and analysis of MB solution during photocatalytic process.

Table S1. Crystallographic Data of **1**.

$[Cu_2 \cdot L \cdot Cl_2]_n$			
Empirical formula	$C_{10}H_8Cl_2Cu_2N_2$	Z	2
Formula weight	354.18	Dcaled, (g/cm^3)	2.141
Temperature (K)	250	*S*	1.66
Wavelength (Å)	0.71073	Limiting indices	$-1 \le h \le 4$; $-15 \le k \le 15$; $-13 \le l \le 14$
Crystal system	Monoclinic	*F*(000)	342.0644
Space group	$P2_1/c$	θ (º)	5.2 to 73.5
a (Å)	3.7727 (7)	Refs collected total / unique	1084 / 919
b (Å)	12.743 (3)	$(\Delta/\sigma)_{max}$	0.001
c (Å)	11.4596 (19)	Data/restraints/paramets	1084/ 0 / 73
α (º)	90	$\mu(mm^{-1})$	8.98
β (º)	94.320 (17)°	Final *R* indices; [I>2(I)]	$R_1 = 0.095$; $wR_2 = 0.253$
γ (º)	90	$\Delta\rho_{max}/\Delta\rho_{min}$	1.72 / -1.2
Volume ($Å^3$)	549.34 (18)	$R_{(int)}$	0.044

Table S2. Selected Bond Lengths (nm) and Bond Angles (°) for **1**.

Bond	Dist. (Å)	Bond	Dist. (Å)	Bond	Dist. (Å)
Cu(1)-C(1C)	2.4186(19)	Cu1-Cl(1B)	2.493(2)	Cu1-Cl(1)	2.2990(19)
Cu(1)-N(1)	1.997 (6)				
Angle	(°)	Angle	(°)	Angle	(°)
N1-Cu(1)-Cl(1)	126.07 (17)	N(1)-Cu(1)-Cl(1C)	106.64 (17)	N(1)-Cu(1)-Cl(1B)	105.18 (17)
C(5)-N(1)-Cu(1)	120.3 (5)	C(1)-N(1)-Cu(1)	122.5 (4)		

Symmetry codes: (A) $-x, -y+1, -z+1$; (B) $-x+1, -y+1, -z+1$; (C) $x-1, y, z$;

Table S3. Characterization and analysis results of N_2 adsorption/desorption isotherms of nanosheets

Parameter	Value	Parameter	Value
Single point surface area	28.2 m^2/g	BET Surface Area	129.2m^2/g
Langmuir Surface Area	765.3 m^2/g	t-Plot External Surface Area	67.3m^2/g
Pore Volume	0.27 cm^3/g	Pore Size	27.4 nm

Table S4. The kinetic investigation for nanosheets, and P_{25}

pH	Kinetics equation	R^2
Photocatalytic degradation of MB by nanosheets of **1**		
3	$\ln(C_0/C_t) = -197.18\ t + 271.25$	0.3725
5	$\ln(C_0/C_t) = -189.43\ t + 241.79$	0.3177
7	$\ln(C_0/C_t) = -1.38\ t + 2.3675$	0.6925
9	$\ln(C_0/C_t) = 0.4554\ t + 0.4666$	0.8749
Photocatalytic degradation of MB by P_{25}		
3	$\ln(C_0/C_t) = -1902.74\ t + 2493.75$	0.2869
5	$\ln(C_0/C_t) = -0.0005\ t + 0.9742$	0.8152
7	$\ln(C_0/C_t) = 0.72225\ t + 0.30524$	0.8894
9	$\ln(C_0/C_t) = 1.05346\ t + 0.03268$	0.9757
Photocatalytic degradation of MO by nanosheets of **1**		
3	$\ln(C_0/C_t) = -197.61\ t + 277.36$	0.3509
5	$\ln(C_0/C_t) = -189.61\ t + 241.82$	0.3178
7	$\ln(C_0/C_t) = -1.511\ t + 2.39103$	0.6915
9	$\ln(C_0/C_t) = 0.40921\ t + 0.5423$	0.8278
Photocatalytic degradation of MO by P_{25}		
3	$\ln(C_0/C_t) = 0.77452\ t + 0.13741$	0.9895
5	$\ln(C_0/C_t) = 1.07025\ t + 0.09851$	0.9769
7	$\ln(C_0/C_t) = 1.06173\ t + 0.07245$	0.9651
9	$\ln(C_0/C_t) = 0.99254\ t + 0.02169$	0.9897

Table S5. The zeta potential vs. pH curves of nanosheets of **1**, and P_{25}

pH	Nanosheets of **1**	P_{25}
3	33.88	18.84
5	21.52	5.81
7	9.43	-7.84
9	-3.21	-22.35

Table S6. Calculation of the frontier electron density of atoms in MB molecules by DFT analysis

Atomic number in MB	$2FED^2_{HOMO}$	$FED^2_{HOMO} + FED^2_{LUMO}$
C(1)	0.0025	0.0937
C(2)	0.0076	0.0780
C(3)	0.0844	0.0525
C(4)	0.0981	0.2257
C(5)	0.0260	0.0167
C(6)	0.0009	0.0799
C(7)	0.0981	0.2258
C(8)	0.0844	0.0525
C(9)	0.0076	0.0780
C(10)	0.0025	0.0934
C(11)	0.0009	0.0799
C(12)	0.0259	0.0167
S(13)	0.0019	0.0009
N(14)	1.4971	0.7485
C(15)	0.0000	0.0171
C(16)	0.0000	0.0171
C(17)	0.0000	0.0171
C(18)	0.0000	0.0171
N(19)	0.0002	0.0217
N(20)	0.0002	0.0216

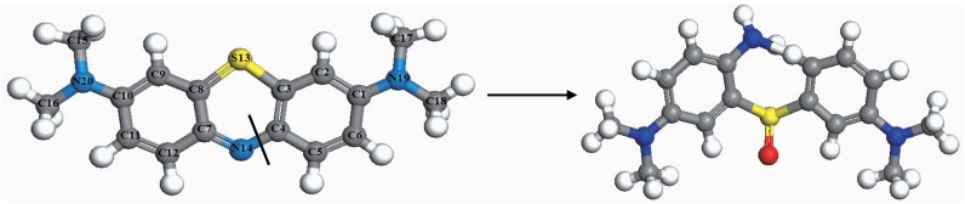

Table S7. Calculation of the frontier electron density of atoms in MO molecules by DFT analysis

Atomic number in MO	$2FED^2_{HOMO}$	$FED^2_{HOMO} + FED^2_{LUMO}$
C(1)	0.0858	0.1376
C(2)	0.1488	0.0859
C(3)	0.0308	0.1156
C(4)	0.2989	0.1525
C(5)	0.0237	0.0822
C(6)	0.1960	0.0982
N(7)	0.0484	0.3723
N(8)	0.2867	0.3800
C(9)	0.0204	0.0798
C(10)	0.0725	0.1275
C(11)	0.014	0.0070
C(12)	0.0937	0.1679
C(13)	0.0006	0.0403
C(14)	0.0677	0.0865
N(15)	0.6912	0.4230
C(16)	0.0032	0.0026
C(17)	0.0035	0.0034
S(18)	0.0038	0.0205
O(19)	0.0058	0.0115
O(20)	0.0092	0.0143
O(21)	0.0158	0.0268